Undulation of Lamellar Crystals of Polymers by Surface Stresses

Ken Taguchi,*,† Yoshihisa Miyamoto,† Hideki Miyaji,‡ and Kunihide Izumi‡

Faculty of Integrated Human Studies, Kyoto University, Kyoto 606-8501, Japan, and Department of Physics, Graduate School of Science, Kyoto University, Kyoto 606-8502 Japan

Received February 17, 2003; Revised Manuscript Received April 21, 2003

ABSTRACT: The periodical striped contrast is observed in the single crystals of isotactic polystyrene and poly(oxymethylene) by transmission electron microscopy. The contrast is attributed to a periodical tilting of the chain stem around the axis normal to the crystal growth plane; the tilting accompanies the surface undulation, which is observed by atomic force microscopy. The wavelength of the undulation increases with the lamellar thickness. In situ observation of the growing crystal by transmission electron microscopy shows that this undulation is introduced during the growth and not through the cooling process of the crystal. It is proposed that the stress of fold surfaces makes a flat lamellar crystal elastically unstable to cause the buckling deformation during the crystal growth.

1. Introduction

The direct observation of isotactic polystyrene (it-PS) single crystals by transmission electron microscopy (TEM) has shown black and white stripe contrast with each stripe line perpendicular to the facets.[1,2] Similar stripe contrasts have been observed also in the single crystals of poly(*p*-xylylene) (PPX),[3] poly(4-methyl-1-pentene) (P4MP), and poly(oxymethylene) (POM).[4] It is to be noted that the stripes have been observed on the surface of lamellar crystals as revealed by atomic force microscopy (AFM) for it-PS1 and for syndiotactic polypropylene (sPP)[5,6] or by TEM with surface replica for it-PS,[7] cellulose triacetate,[8] and xylan.[9]

It has been suggested that the bands in the stripe contrast correspond to crystal domains; the chain stems in neighboring bands tilt in the growth plane alternately. For the solution-grown POM and P4MP crystals, Bassett et al. have attributed this tilting to the hollow-pyramidal shape of these lamellae in solution as in the case of PE;[4] nonplanar pyramidal lamellae are sheared to flatten on a substrate when they are deposited from their suspension. However, the same are observed even in the it-PS crystals grown from the melt;[1] no sheared deformation is expected in this case. As such we need to search for another structure and origins for the stripe pattern.

In this paper are reported the details of the stripe contrasts in TEM images and the surface topography examined with AFM of melt-grown it-PS crystals. TEM observation of solution-grown POM and in situ observation of the growth of it-PS crystals from melt are also reported. On the basis of these observations, we propose a new structure for the stripe pattern and discuss its origin.

2. Experimental Section

The samples used for this study were it-PS purchased from Polymer Laboratory (M_w = 590 000, M_w/M_n = 3.4, tacticity: 97% isotactic triad) and POM (Derlin 500 NC-10).

* Corresponding author. Fax: (+81)75-753-6805. E-mail: taguchi@phys.h.kyoto-u.ac.jp.
† Faculty of Integrated Human Studies, Kyoto University.
‡ Department of Physics, Graduate School of Science, Kyoto University.

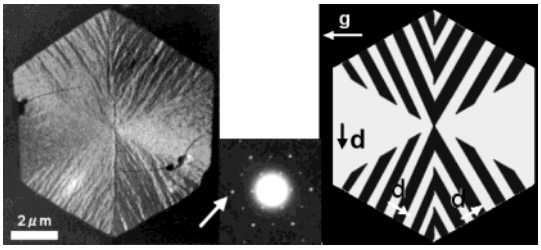

Figure 1. TEM dark field image with the 220 reflection (left) and the electron diffraction pattern (middle) of an it-PS single-crystal grown from the melt at 210 °C. Right: Schematic picture of the stripe contrast and reflection vector, *g*, displacement vector, *d*, in each sector.

Thin films of it-PS (ca. 10 nm thick) were prepared by spin coating a 0.4−0.7 wt % cyclohexanone solution at 4000 rpm on a carbon-evaporated mica.[10,11] The films were melted at 250 °C for a few minutes, quenched to room temperature in order to increase crystal nuclei, and immediately elevated to a crystallization temperature, 210, 195, or 180 °C in a hot stage (Mettler FP800). The films crystallized isothermally were again quenched to room temperature. These samples were investigated at room temperature by TEM (JEOL 1200EX II) operated at 120 kV and by AFM (SHIMADZU SPM-9500 J) in the contact mode. In situ observation of the growth of it-PS crystals by TEM was performed at 210 °C. POM single crystals were grown from 0.1 wt % bromobenzene solution by slow cooling (1 °C/min) from the boiling temperature (156 °C) to room temperature. The POM single crystals deposited on a carbon film were observed by TEM at −120 °C to minimize the radiation damage by electrons.

3. Results

Figures 1 and 2 show the dark field images of it-PS single crystals grown from the melt at 210 °C and a solution-grown POM single crystal, respectively. The electron diffraction shows that both the crystals have the single crystalline orientation with chain axis almost perpendicular to the lamellar surface. However, the dark field images indicate the crystals are not really single crystals but consist of six triangle sectors with many parallel bands. The bands in a sector are nearly normal to the growth face {110} for it-PS and {100} for POM and aligned with an almost constant spacing. The bands are visible in four sectors of six but not in the other two sectors with growth faces parallel to the diffracting plane, while in the bright field images they

10.1021/ma034201+ CCC: $25.00
Published on Web 06/14/2003

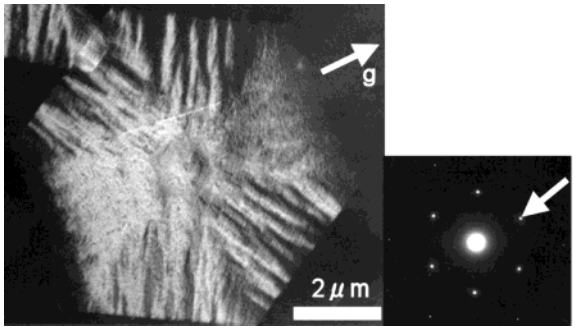

Figure 2. TEM dark field image and electron diffraction pattern of a POM single-crystal grown from the solution. The diffraction spot, 100, used for this image is shown by the arrow.

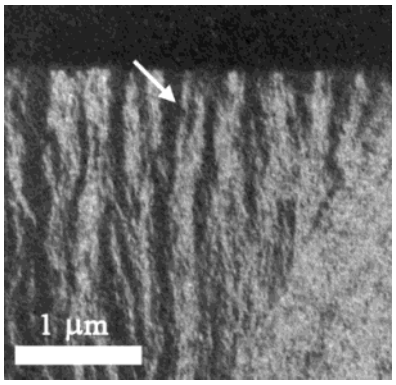

Figure 3. Details of stripe contrast of Figure 1. The boundaries of each band are not clear and are not straight lines either. Fine streaks can be found in a band. Some bands split off toward growth face as shown by an arrow.

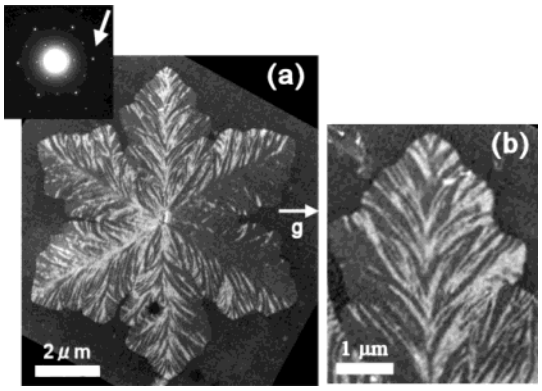

Figure 4. TEM 220 (shown by arrow) dark-field image of an it-PS dendritic crystal grown at 195 °C in an ultrathin film 10 nm thick: (a) a whole crystal; (b) a magnified view of the upper part of image a.

are visible in all sectors.[1] Hence the displacement vectors, $\vec{d}$, which contribute to the diffraction contrast have only the component parallel to the growth face in each sector but not parallel to the *c*-axis. A band occasionally splits into two as shown in Figure 3, and the contrast of the band is not uniform but shows fine structure.

Crystals of it-PS grown in ultrathin films (ca. 10 nm) form dendrites with curved growth faces.[10] Figure 4 a shows the TEM images of a dendritic lamella grown at 195 °C in a 10 nm ultrathin film. Although the stripe contrast similar to those in the faceted crystals appear in the dendrite, they are not perpendicular to the crystallographic {110} plane but curve so as to be normal to the growth faces of the dendrite; the bands advance along the growth direction. The bands can be

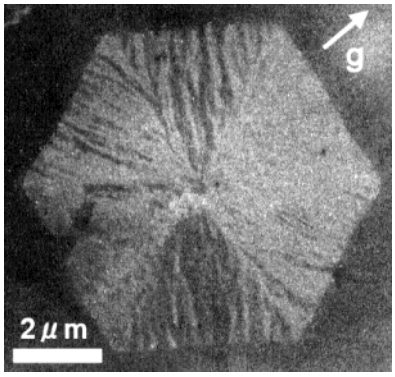

Figure 5. In situ dark field image with 220 reflection of an it-PS crystal growing at 210° in TEM.

here observed in the noncontrast sectors of the faceted crystal, indicating that $\vec{d}$ is no longer parallel to the {110} planes but is always parallel to the growth face. The splitting of a band is also frequently observed at 195 °C as shown in Figure 4b.

Figure 5 shows an in situ TEM image of an it-PS crystal growing at 210 °C. Since the stripe pattern is clearly observed in the image, the bands have been already introduced during crystal growth, and hence, we can discard the possibility that those are formed in the quenching process.

To determine the lattice distortion which gives the stripe contrast in the TEM image, the variation of the contrast with the tilt of a crystal around the [$\bar{1}$10] axis has been investigated. Figure 6 shows the successive dark field images of an it-PS crystal of Figure 1 with an interval of a tilting angle of 2° around the [$\bar{1}$10] axis, which is normal to the reflecting vector as shown in the figure. The bands shift the positions gradually and reverse the contrast at about 6° of tilt (Figure 6, parts b and e); the bright bands in part b turn into the dark ones in part e and vice versa. The bright band in part a grows broader gradually through part b to part c and then splits into two narrower bands in part d, and finally, in part e, those split bands join together to give the contrast reverse to part a; the boundaries of bands move with crystal tilt, and each bright band splits before the contrast is reversed. The process does not occur simultaneously in all bands, and the width and spacing of those bands change inhomogeneously during the tilt: The similar process in tilting has been also observed in POM single crystals.

Figures 7 and 8 show the surface topography obtained by AFM for it-PS crystals grown in the ultrathin films[10] at 210 and 195 °C, respectively. The stripes perpendicular to the growth face are clearly observed in all the six sectors of both the crystals. The height profile in Figure 7b shows that the lamellar crystal has a wavy, undulated surface with a height amplitude of about 1 nm. In Table 1 are shown the mean spacing of the bands in TEM images λ_t and that in AFM images λ_a at three crystallization temperatures, T_x (180, 195, and 210 °C). The two spacings agree well each other at those temperatures. Therefore, we conclude that the lattice distortions observed by the dark field image accompany the surface undulation. The spacing λ decreases with lowering T_x. In Figure 9, the spacing is plotted against $1/\Delta T$, where $\Delta T = T_m - T_x$ represents the supercoolings of the crystal growth (T_m is melting temperature, 242 °C).[12] Since the lamellar thickness l depends on the supercooling of crystal growth ΔT as $l = (\alpha/\Delta T) + \delta l$,[13]

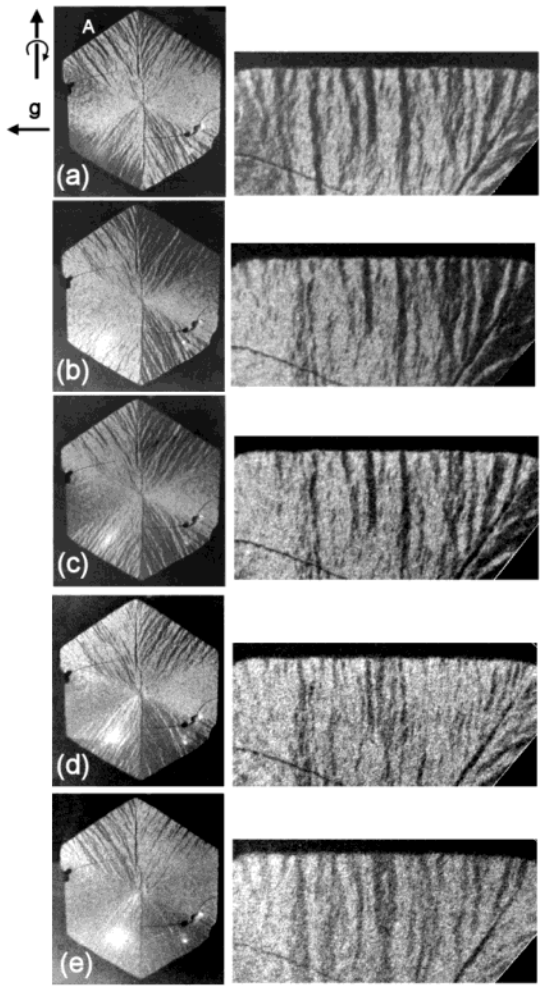

Figure 6. Variation of stripe contrast of an it-PS crystal of Figure 1 with increasing tilt angle every 2° from part a to part e. The magnified image of sector A is shown in right-hand side of each image. A vertical arrow at left side of part a represents the axis of the tilt, [110], and a horizontal one the 220 reflection vector.

where α and δl are constants, the spacing of the bands increases with the lamellar thickness, neglecting δl of the small value.

4. Discussion

The undulation of a lamellar crystal, i.e., the origin of the stripe pattern in TEM, should be caused by the tilt of chain stems in the lateral growth planes as has been discussed by several authors;[1,2,4] the tilt alternates its direction in neighboring bands. The inhomogeneous contrast observed within a band indicates that the tilt is not uniform even in one band. The stripe contrast has been also observed in the TEM images of solution-grown PE crystals, where the contrast corresponds to the domain structure, which is caused by collapse of the hollow pyramidal crystal, and the stems tilt homogeneously in one domain as shown schematically in Figure 10a. Such a domain structure give the stripe pattern in TEM, however, it cannot cause the displacement of the boundaries of stripe contrast during the crystal tilting as shown in Figure 6. The displacement of the contrast indicates that the stem tilting should be gradual and continuous in the lateral growth faces, and hence, the boundaries of domains cannot be defined. The structural model of the undulated lamellar crystal is shown in Figure 10b. The lamella is deformed sinusoidally keeping the chain directions perpendicular to the lamellar surface; the chain axis tilts accordingly. Because of finite thickness of the crystal the reciprocal lattice point ($hk0$) elongates along the c^* axis. The intensity of the diffracted beam is accordingly appreciable over ~2° of crystal tilting in the present case.[14] This undulated lamellar crystal gives the "split and reversal" of the stripe contrast (Figure 11); hatched areas represent the regions where the reflection condition is not satisfied, and hence the striped contrast show the "split and reversal" with the tilting of crystals.

Table 1. Growth Temperature T_x, vs Spacing of Bands λ_t by TEM and λ_a by AFM

T_x (°C)	λ_t (10^2 nm)	λ_a (10^2 nm)
210	2.6 ± 0.4	2.6 ± 0.5
195	1.9 ± 0.3	1.8 ± 0.2
180	1.4 ± 0.2	1.4 ± 0.2

For the undulated lamella formed in the crystal growth, we propose "buckling" model. A well-developed polymer lamellar crystal could be regarded as a very thin crystal sandwiched between fold layers as shown in Figure 12a. Because of the disordered molecular packing, the density of the fold layers is lower than that of the crystal part. The fold layers are therefore under substantial compressive stress through the crystal part due to the chain connectivity. The system of the stressed thin fold layer and crystal becomes mechanically unstable and buckle sinusoidally when the magnitude of the stress becomes larger than a critical value deter-

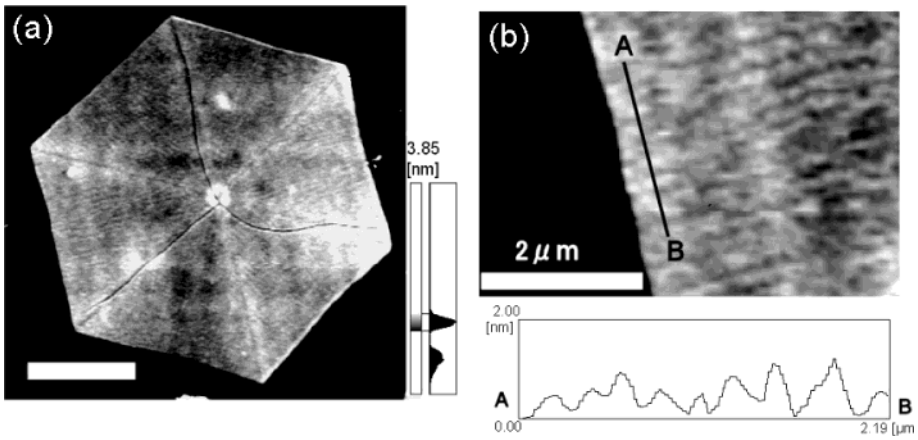

Figure 7. (a) AFM image of the lamellar surface of an it-PS crystal grown in ultrathin films at 210 °C and (b) the magnified image with surface height profile of line A−B.

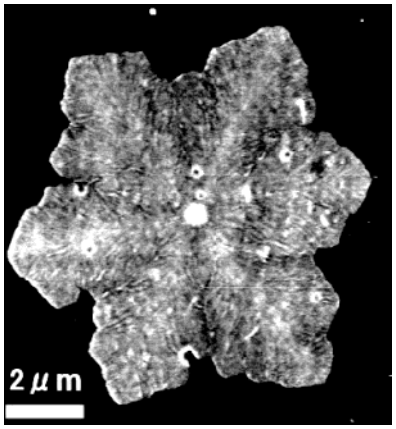

Figure 8. AFM image of the lamellar surface of an it-PS dendritic crystal grown in ultrathin films at 195 °C.

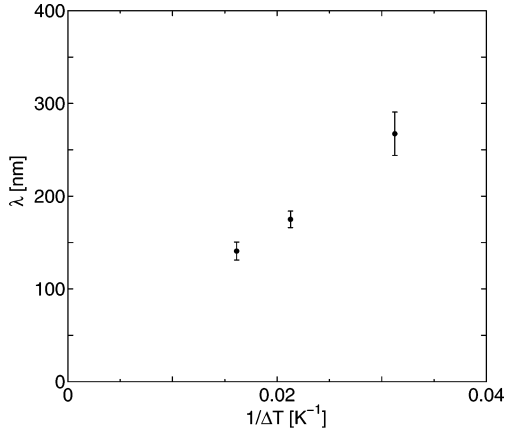

Figure 9. Spacing of the bands λ vs inverse of supercooling $1/\Delta T = 1/(T_m - T_x)$, where T_m is the melting temperature, 242 °C,[12] and T_x the crystallization temperature, 180, 195, and 210 °C.

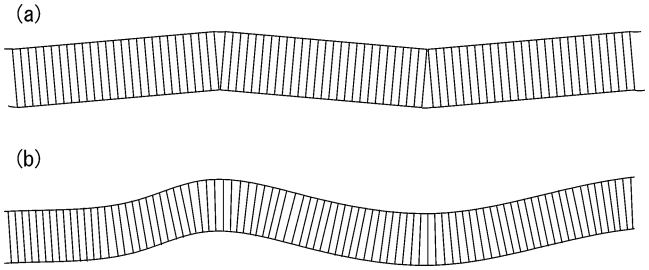

Figure 10. Schematic illustrations of lamellar structure viewed from the lateral growth face. The short lines represents the chain stems. (a) Domain structure model of chain tilt in the case of collapsed nonplanar lamellae. The chain stems are tilted against the lamellar normal. (b) Undulated lamellar model. The lamella are deformed sinusoidally with chain stems normal to the local lamellar surface and tilted periodically.

mined by the size, form and elastic moduli of the lamella. For a thin square plate with b in length and l in thickness, sandwiched between compressed layers of thickness t on both sides, the critical stress needed to initiate buckling is given by[15]

$$P_{cr} \sim \frac{k\pi^2 D}{b^2(2t)} = \frac{k\pi^2}{12(1-\nu^2)}\left(\frac{El^3}{2b^2 t}\right) \qquad (1)$$

where k is 4 for a square plate, E is the Young modulus, ν is the Poisson ratio and $D = El^3/12(1-\nu^2)$ represents the flexural rigidity of the plate. This expression of

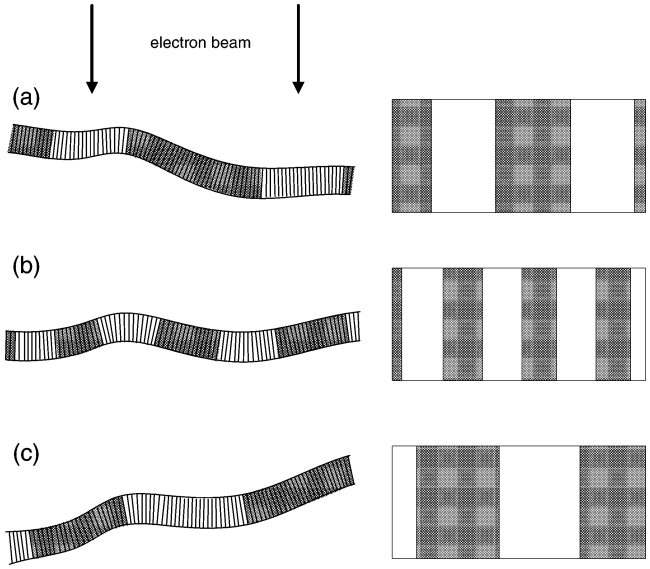

Figure 11. Schematic representation of the variation in the stripe contrast with the tilt of the undulated lamella from part a to part c, which are the cross section viewed from the [110] tilting axis. The diffracting region with stems nearly parallel to electron beam are represented by bright contrast in both cross-sectional views (left) and top views (right); short lines in the lamella represents chain molecules and the traces of the reflecting plane. The reversal of the stripe contrast between parts a and c, and the split of each band in part b are shown.

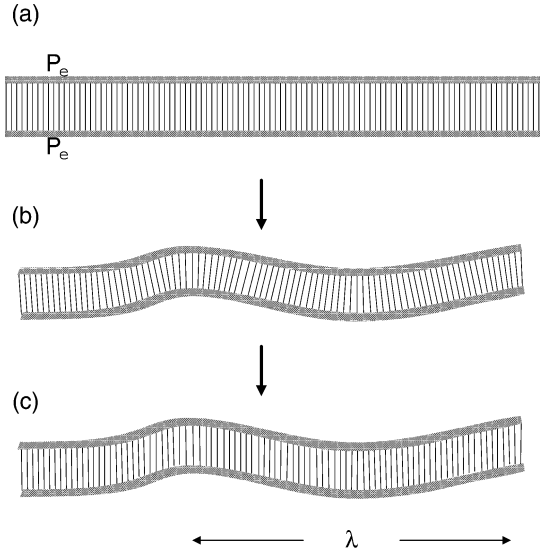

Figure 12. Schematic illustration of buckling deformation and relaxation after it. (a) Cross-sectional view of the lamella crystal sandwiched between stressed fold layers (P_e). (b) Lamella deformed elastically into sinusoidal form after buckling with periodical tilts of stems. (c) Lamella with parallel stems after the rearrangement of folds by chain sliding.

critical surface stress corresponds to the one which was already estimated for the lamellar twisting by Hoffman and Lauritzen.[16] In the crystal growth, the value of b of a lamella in eq 1 becomes larger and larger, and hence the critical stress, P_{cr}, becomes eventually smaller than a fold surface stress P_e. The lamella should buckle accordingly. Here exists a critical width, b_{cr}, at which the P_{cr} is equal to the P_e. After the lamella has buckled, each crystallizing chain should attach parallel to the tilted stem at the growth face and the tilts of stems remain almost constant along the growth direction keeping the bands normal to the growth face. We here assume that this b_{cr} corresponds to the wavelength of

buckling λ, i.e., the band spacing observed. Accordingly, at the critical width

$$P_e = P_{cr} \propto \frac{l^3}{2b_{cr}^2 t} \quad (2)$$

$$\propto \frac{l^3}{2\lambda^2 t} \quad (3)$$

hence

$$\lambda \propto \sqrt{\frac{l^3}{2tP_e}} \quad (4)$$

If P_e and t of compressed fold layers are assumed to be almost constant irrespective of lamellar thickness, this equation indicates a positive dependence of λ on l, which is observed in Figure 9. The wavelength in the pattern of buckling deformation of such a thin plate with compressed surface layer is generally to be proportional to its thickness, as observed in thin films of metals supported on an elastomeric polymer.[17] Furthermore, the P_{cr}, calculated roughly from the values observed, l and λ ($\sim b$), and appropriate constants, E and v,[18] is in fact of the same order of magnitude, several hundred megapascals, as the compressive stress of the fold layer estimated from the E and the density difference between amorphous and crystal phases. Since the folding characteristic of polymer crystals is believed to occur mainly along the each lateral growth face,[13] in particular for faceted single crystals, the undulations observed along each growth face indicates that the stress causing the buckling deformation could be originated from the folds of chain molecules at both the surfaces of lamella. It also has been proposed that lamellar twisting in banded spherulites are caused by the stresses within the fold layers; internal stresses on both sides of such a thin plate could make itself mechanically unstable and twist[16,19] or cause spiral dislocations with same sense.[20,21] For the lamellar twisting, a kind of chirality is required, and hence for polyethylene, nonchiral molecules, uniform chain tilting to the lamellar normal was proposed to result in the shear stress at opposite fold surfaces, together with the strain at sector boundary.[19,22] It has been pointed out by Keith and Padden that in the absence of chain tilt to lamellar normal, such surface stress would be of small consequence to twisting of lamellae, except perhaps that unmatched fluctuations might cause wrinkling in otherwise flat crystal.[19] It should instead be noted here that it-PS crystals have no chain tilting. It means that the main part of the stress is uniaxial, along the growth face and hence induces the undulated lamellae by buckling. In fact, the spherulites of it-PS and P4MP are usually known to be nonbanded.[23]

Since the buckling deformation should occur in the direction of the maximum stress, the undulation parallel to growth face in Figures 1, 2, and 4 indicate that the direction of the maximum stress in the fold layer is parallel to the growth face. Therefore, it can be concluded that the molecular chains would principally fold back in the lateral growth face, whether it is faceted (Figures 1 and 2) or not (Figure 4). Although the fold surface stress was assumed to be uniform and parallel to growth face and equal at opposite fold surfaces so far, there should be inhomogeneity in both the magnitude and the direction due to the fluctuation of folding during the growth. This inhomogeneity in fold surface stresses causes inhomogeneous buckling deformation, and hence, the contrast within a band is not uniform and boundaries are not straight as observed in Figure 3. The split of a band near the growth face in Figure 3 can be due to a twisting of the lamella by a few degrees toward the growth face as depicted in Figure 13; the direction of the lamellar normal changes gradually along the growth direction and hence the diffracting regions represented by hatched area show the split of a band. This twist might also be attributed to differences in stress at opposite fold surfaces.[19,22,24]

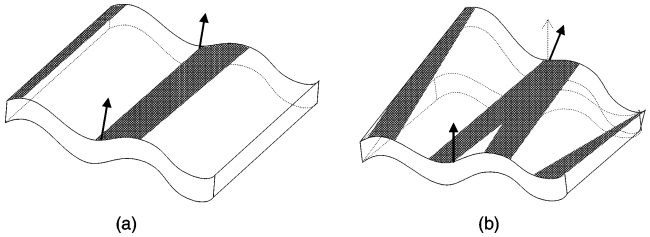

Figure 13. Schematic 3-D illustrations of the undulated lamella tilted to the electron beam (a) without twisting and (b) with twisting toward growth face as shown by the 13 arrows, lamellar normals. The hatched areas represent diffracting regions, producing the split band in part b.

If the molecular rearrangement could be easy in the crystal and the fold surface, there would disappear the periodical tilt of stems as schematically shown in Figure 12, parts b and c. The polymers reported so far to show the stripe contrast in the single crystals are it-PS, PPX, POM, P4MP, cellulose triacetate, and xylan. These polymers are rather stiff polymers with a large characteristic ratio, C_∞, and hence are difficult to slide along the chain directions and to rearrange within the crystal. Among those polymers, it-PS and P4MP form nonbanded spherulites[23] and have little chain tilts against the lamellar normal. Therefore the lamellar single crystals of those polymers forming nonbanded spherulites tend to buckle and form the undulated lamellae.

5. Conclusion

In this paper, we have found that the stripe contrast in the TEM images of it-PS and POM single crystals are due to the undulated lamella; the stems in the crystal tilt in the growth face sinusoidally during crystal growth. The wavelength of the undulation increase with the lamellar thickness. We propose that the stressed surface fold layers, which are characteristic of polymer crystals, make the thin flat lamella elastically unstable and cause the buckling deformation, leading to the undulated lamellar structure along the growth face. The direction of this buckling deformation along the growth face suggests that the molecular chains mainly fold back in the growth face even in the melt-grown crystals without facets. This buckling deformation should occur only for the polymer single crystals which have symmetrical fold surface stress in both sides, while for the crystals with unsymmetrical fold stresses at opposite sides due to a kind of chiral factor such as chain tilt to lamella normal, the lamellar should twist as has been observed in banded spherulites.

Acknowledgment. This work was supported partly by Grant-in-Aid for Science Research on Priority Areas, "Mechanism of Polymer" Crystallization (No. 12127204)-

from The Ministry of Education, Science, Sports, and Culture, Japan.

References and Notes

(1) Sutton, S. J.; Izumi, K.; Miyaji, H.; Miyamoto, Y.; Miyashita, S. *J. Mater. Sci.* **1997**, *32*, 5621−5627.
(2) Izumi, K.; Gan, P.; Hashimoto, M.; Toda, A.; Miyaji, H.; Miyamoto, Y. Nakagawa, Y. In *Advances in the Understanding of Crystal Growth Mechanisms*; Nishinaga, T., Nishioka, K., Harada, J., Sasaki, A., Takei, H., Eds.; Elsevier Science: Amsterdam, 1997; p 337.
(3) Tsuji, M.; Isoda, S.; Ohara, M.; Kawaguchi, A.; Katayama, K. *Polymer* **1982**, *23*, 1568−1574.
(4) Bassett, D. C.; Dammont, F. R.; Salovey, R. *Polymer* **1964**, *5*, 579−588.
(5) Tsukruk, V. V.; Reneker, D. H. *Macromolecules* **1995**, *28*, 1379−1376.
(6) Tsukruk, V. V.; Reneker, D. H. *Phys. Rev. B* **1993**, *51*, 6089−6092.
(7) Bassett, D. C.; Vaughan, A. S. *Polymer* **1985**, *26*, 717−725.
(8) Manley, R. St. J. *J. Polym. Sci.* **1963**, *1A*, 1875.
(9) Marchessault, R. H.; Morehead, F. F.; Walter, N. M.; Gludemans, C. P. J.; Timell, T. E. *J. Polym. Sci.* **1961**, *51*, S66−68.
(10) Taguchi, K.; Miyaji, H.; Izumi, K.; Hoshino, A.; Miyamoto, Y.; Kokawa, R. *Polymer* **2001**, *42*, 7743−47.
(11) Taguchi, K.; Miyaji, H.; Izumi, K.; Hoshino, A.; Miyamoto, Y.; Kokawa, R. *J. Macro. Sci. Phys.* **2002**, *41*, 1033−1042.
(12) Suzuki, T.; Kovacs, A. J. *Polymer* **1970**, *1*, 82.
(13) Hoffman, J. D.; Davis, G. T.; Lauritzen, J. I., Jr. In *Treatise on Solid State Chemistry 3*; Hannary, N. B., Eds.; Plenum Press: New York, 1976; Chapter 7, p 497.
(14) Hirsch, P. B.; Howie, A.; Nicholson, R. B.; Pashley, D. W.; Whelan, M. J. *Electron Microscopy of Thin Crystals*; Butterworth: London, 1965; Chapter 7, p 156.
(15) Timoshenko, S. P.; Gere, J. M. *Theory of Elastic Stability*; McGraw-Hill: New York, 1961; Chapter 9, p 348.
(16) Hoffman, J. D.; Lauritzen, J. I. Jr. *J. Res. Natl. Bur. Stand. (U.S.)* **1961**, *65A*, 297.
(17) Bowden, N.; Brittain, S.; Evans, A. G.; Hutchinson, J. W.; Whitesides, G. M. *Nature* **1998**, *393*, 146−149.
(18) Rudd, J. F. In *Polymer Handbook*, 3rd ed.; Brandrup, J., Immergut, E. H., Eds.; Wiley-Interscience: New York, 1989. Ch. V.
(19) Keith, H. D.; Padden, F. J., Jr. *Macromolecules* **1996**, *29*, 7776−7786.
(20) Toda, A.; Keller, A. *Colloid Polym. Sci.* **1993**, *271*, 328−342.
(21) Toda, A.; Arita, T.; Hikosaka, M. *Polymer* **2001**, *42*, 2223−2233.
(22) Owen, A. J. *Polymer* **1997**, *38*, 3705−3708.
(23) Geil; P. H. *Polymer Single Crystals*; Interscience: New York, 1963.
(24) Keith, H. D.; Padden, F. J., Jr. *Polymer* **1984**, *25*, 28−42.

MA034201+